International Journal of Concrete Structures and Materials

RESEARCH Open Access

Energy-Based Approach for Studying Fibre-Reinforced Concrete Subjected to Impact Loading

Petr Konrád* and Radoslav Sovják

Abstract

In general, concrete behaves differently when the load is applied at a different speed, i.e. concrete's mechanical parameters are strain-rate sensitive. There is a need for an experimental method that should meet several criteria such as removal or accurate description of boundary conditions, simplicity, affordability and reproducibility of the experiments. The main goal of this study is the design, assembly and optimisation of the experimental apparatus and procedure to carry out the impact testing. Using this apparatus, an experimental study was conducted. The main aspect of this experimental method is the elimination of rigid supports, which could negatively affect the obtained results. Measured data are acquired using specifically designed measuring devices and analysed using a computer script. Four concrete mixtures were examined ranging from high-strength concrete to ultra high-performance concrete. Quasi-static experiments were also carried out for comparison. A clear difference in quasi-static and impact performance of the materials was observed. Different trends for different compositions of the tested concrete specimens were apparent. Higher fibre content specimens generally showed higher strain-rate sensitivity and the highest strain-rate sensitivity was observed in combination with the two strongest concrete matrices. This was most probably related to fibre anchoring, as complete fibre pullout before premature matrix failure was critical. The newly designed measuring apparatus greatly improves the speed and precision of conducting the impact experiments. It can be successfully used for a relatively quick and simple comparison of materials when designing concretes for withstanding elevated strain-rate loading.

Keywords: concrete, fibre, energy, strain rate, impact, pendulum

1 Introduction

Mechanical characteristics of concrete, in general, are strain-rate sensitive. Different values of certain mechanical characteristics can be observed when the load is applied at different speeds. This phenomenon has been extensively studied and several conclusions have been drawn (Cao et al. 2019; Min et al. 2014; Othman and Marzouk 2016; Pajak 2011; Vegt and Weerheijm 2016; Xu et al. 2016; Yoo et al. 2019). However, a general consensus or standardisation regarding this kind of testing is still insufficient. Studies reporting the results of concrete's performance subjected to elevated strain-rate loading are using different experimental methods, setups and techniques (Wu et al. 2015; Vivas et al. 2020; Sadraie et al. 2019; Heravi et al. 2020; Khosravani and Weinberg 2018; Tran and Kim 2012). Since the tested specimens are loaded dynamically, it is important to take into consideration the inertial forces of not only the specimen, but also the testing mechanism and connected measuring equipment. A finite velocity of the stress waves will also become important, unlike in the quasi-static experiments where we can afford to neglect these effects in most cases. This means, that certain experimental results

*Correspondence: petr.konrad@fsv.cvut.cz
Faculty of Civil Engineering, Experimental centre, Czech Technical University in Prague, Thákurova 7, Prague 6 16629, Czech Republic
Journal information: ISSN 1976-0485 / eISSN 2234-1315

might not reflect the true response of the specimen (Bede et al. 2015; Ožbolt et al. 2014). Overall, the dynamic loading problem should be approached without the assumptions related to the quasi-static loading.

One of the most problematic aspects of most experimental principles, especially the drop-weight techniques, are the boundary conditions and data acquisition. The drop-weight principles usually resemble the quasi-static conditions, where a beam specimen is supported by two rigid supports on its sides, with the load being applied in the centre of the span. As the name suggests, the load is formed by a falling weight with various shapes and sizes. If the specimen is just resting on the supports, then it can rebound, which negatively affects the acquired force measurements. This led researchers to fix the specimens to the supports using various mechanisms, which only complicates the definition of the boundary conditions more. In all cases, however, it is not clear how much mechanical energy is dissipated by the supports or the overall structure of the apparatus, i.e. how much are the results influenced by the experimental setup.

The drop-weight principle is of course not the only possible technique to study concrete at elevated strain rates, but despite its flaws, it presents several major advantages. The most important are the ability to use practically any specimen size and geometry as the principle is easily scalable, relative simplicity and affordability of the apparatus and the ability to perform the experiments quickly. The first advantage is especially important to achieve a representative volume for fibre-reinforced concrete so the fibres would not show preferential orientation along the sides (wall effect). The other advantages are necessary when conducting a comparative study using a large group of specimens when conducting basic parametric research regarding the material composition to optimise the overall design.

The aim of this study was to improve the known drop-weight principle by eliminating the fixed supports, moving towards an energy-based approach (compared to displacement-force approaches) and introducing a new data acquisition system. The motivations for these improvements include lowering the influence of the experimental setup on the results thus improving accuracy and reproducibility and significantly improving the speed at which the experiment can be conducted and analysed. Last but not least, the whole system should be relatively simple to limit the number of variables and keep its cost reasonably low. In a second step, the aim was to evaluate the system by conducting a series of experiments using various fibre-reinforced concretes. The motivation was to not focus on one particular type of concrete, but test several significantly different types to observe their different performance when subjected to testing in the framework of one study, using one experimental approach, which is uncommon in literature sources, such as described above.

2 Design of the Experiments

2.1 Test Principle

It is possible to improve the drop-weight technique using key changes to an already existing impact pendulum machine. This machine uses a steel impactor that strikes a beam concrete specimen, placed perpendicularly against it. The first change is the elimination of all rigid supports of the specimen in the direction of the applied load. This principle was used by Yu et al. (2016). This changes the whole experiment from the classic force–displacement to the mechanical energy approach, i.e. we will be analysing the mechanical energy dissipated by the specimen. Even though it is not supported, its mass will create significant inertial forces to react to the load. Therefore, dissipation will occur because the specimen will be damaged by the impact.

The impact pendulum machine is shown in Figs. 1 and 2. The impactor and the specimen are free to move, which means that the measuring principle is based on the tracking of their movements. At the core of this approach is a simple energy balance equation

$$E_{Ai} = E_{I.pre} - E_{I.post} - E_{S.post}, \tag{1}$$

where E_{Ai} is the mechanical energy dissipated after one impact, $E_{I.pre}$ is the energy input into the experiment - the initial energy of the impactor before the impact, $E_{I.post}$ is the impactor's energy after the impact and $E_{S.post}$ is the specimen's energy after the impact. This principle can only be used for impacts after which the specimen remains in one piece (it did not fail yet). Since this experiment aims to obtain the overall dissipated energy until failure, the specimen must be impacted multiple times. The overall dissipated energy is then calculated as

$$E_A = \sum_{i=1}^{n} E_{Ai}, \tag{2}$$

where n is the number of last but one impact, i.e. excluding the last impact after which the specimen completely failed. This introduces a minimal inaccuracy of the results, as will be shown later. The following text will thoroughly describe the various elements of the experimental apparatus and introduce the specific measuring techniques to obtain the energy balance equation's terms.

2.2 Experimental Apparatus

Both the steel impactor and the tested specimen are suspended on steel ropes. The design keeps the impactor in a horizontal position at all times, which can be seen in

Fig. 1 The whole impact pendulum.

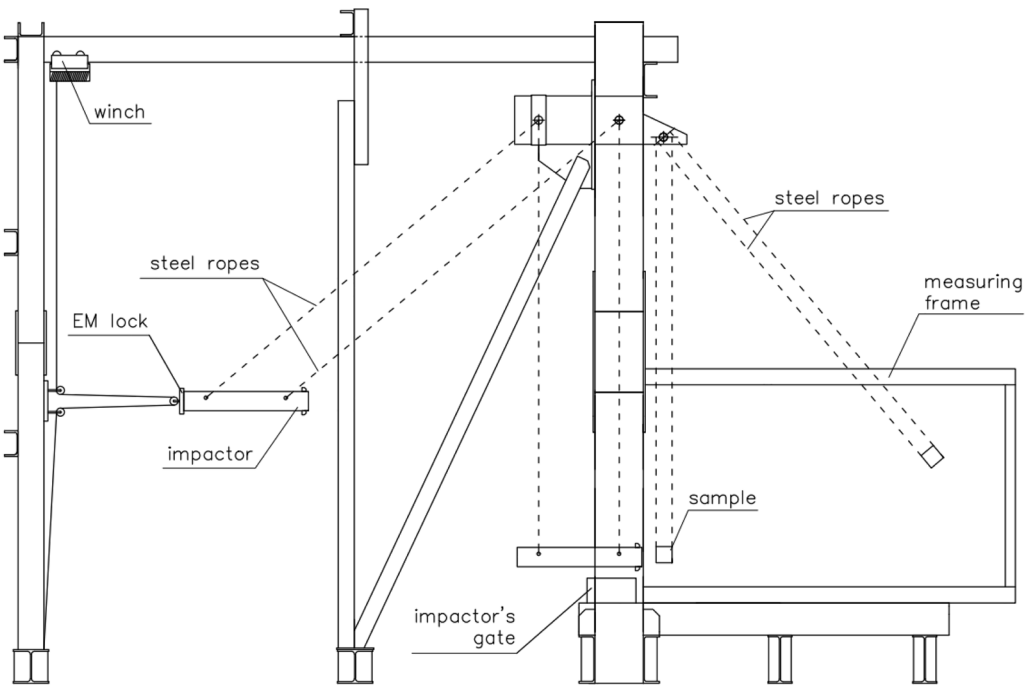

Fig. 2 The schematic of the impact pendulum.

Fig. 2. The main body of the impactor is made of a solid block of ordinary construction steel, but the front part is a removable cylinder made of hardened steel (hardness HRC 55). Dimensions of the impactor are 775 mm × 120 mm × 50 mm. Fig. 3 shows a comb-like measuring attachment on one side of the impactor. On the opposite

Fig. 3 The measuring attachment of the impactor.

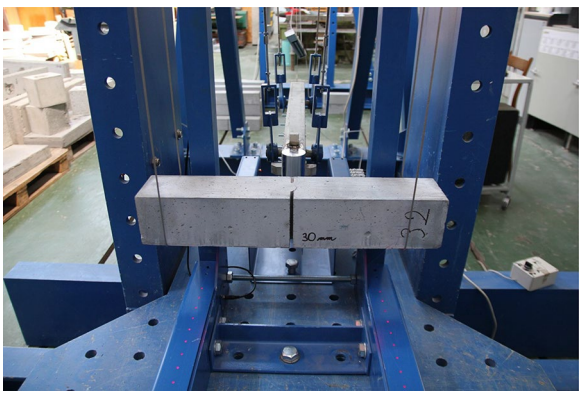

Fig. 4 The specimen resting in the loops formed by the steel ropes.

side of the impactor, there is a counterweight to this attachment to not offset the centre of mass. Lifting the impactor is done using an electric winch, which is connected to the back of the impactor with an electromagnetic lock. This allows for an easy release of the impactor from a predetermined height. The structure of the impact pendulum is made stiff enough to provide sufficient support to the impactor as it moves.

The specimen's dimensions are 100 mm × 100 mm × 550 mm. The impactor strikes the specimen in its centre along its entire height (Fig. 4). The specimen is simply resting inside loops formed by the two steel ropes to simplify the mechanism and limit the possible influences of more attachments. All of the ropes are connected to rotating mechanisms, to limit energy losses. On a side note, it has been confirmed in a similar work regarding the impact of glass plates, that the steel rope suspension has a negligible effect on the specimen's behaviour during this type of impact testing (Janda et al. 2020).

On the right side of the schematic in Fig. 2, there is a steel table that forms a support for various equipment. In this case, there are two measuring frames to conduct position tracking of the specimen, and a smaller optical gate for the impactor. The comb-like attachment on the side of the impactor works together with this smaller gate. The equipment is designed to not obstruct the movement of both objects. All measuring equipments will be described later in more detail. The whole structure of the impact pendulum is firmly attached to the concrete floor.

2.3 Measuring Technique—Impactor

The mechanical energies of both objects from the balance Equation 1 can either be potential or kinetic energies defined as

$$E_{pot} = mgh, \tag{3}$$

and

$$E_{kin} = \frac{1}{2} J\omega^2, \tag{4}$$

respectively, where m is the mass of the impactor, g is the gravitational acceleration, h is the height, J is the moment of inertia and ω is the angular velocity. It is important to note, that for higher accuracy, both pendulum systems (impactor and specimen) must not be simplified as an infinitely small object suspended on a massless cord. The aforementioned quantities describe the whole systems (the rotating mechanisms, cables, attachments, etc.), which must be more carefully analysed, especially their moments of inertia.

At the start of the experiment, the impactor's vertical position relative to the floor is measured. The electromagnetic lock is then activated to pull the impactor to a certain predetermined position, which is also measured relative to the floor. Both of these measurements need to be recalculated to the heights of the centre of mass of this pendulum system. Their difference is the initial height used to calculate the initial mechanical (potential) energy for the energy balance equation. From this position, the impactor is released. Right before it strikes the specimen in the lowest part of its trajectory, all of the mechanical energy is transformed into kinetic energy. It was confirmed by high-speed camera measurements that energy losses from the movement are negligible. This means, that we can also measure the impactor's velocity at this point to calculate its kinetic energy and have both it and the potential energy for additional control and higher accuracy (energies can be averaged, for example).

Fig. 5 shows the smaller optical gate device, which works together with the comb-like attachment on the impactor. The attachment has a precise laser-cut geometry with holes. The gate consists of pairs of six laser modules, that aim at six photodiodes. Each pair outputs

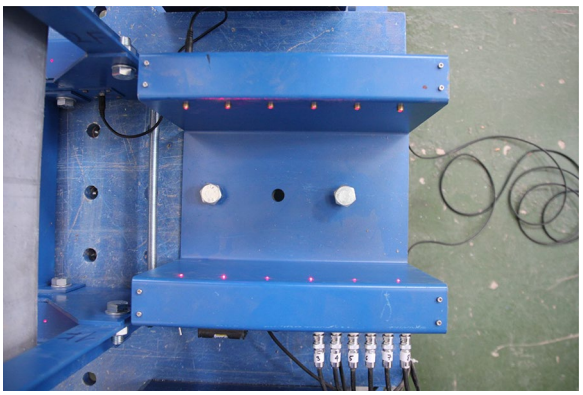

Fig. 5 The smaller optical gate device for tracking the impactor.

a separate voltage signal depending on the illumination state of the photodiode. If a laser beam is uninterrupted (it illuminates the photodiode) then a high-level voltage signal is acquired. If the impactor's attachment blocks the beam, then a low-level signal is seen. The voltage is provided by a battery source. Six separate measurements are acquired from these six pairs, which allows us to average them for higher accuracy.

Fig. 6 shows a typical measured signal from one photodiode. Note the sudden change in frequency of the signal, which corresponds to the time of impact and deceleration of the impactor. Time points are identified at each point of the signal, where it crossed the average voltage value between the high and low states. These time points can be paired with the geometry of the holes of the attachment to calculate partial velocities, which can be seen in Fig. 7. The time of impact is clearer here. The before-impact velocity of the impactor can be calculated as an average of a few values before the impact, in this case, 10. This final velocity needs to be recalculated into the angular velocity of the impactor's pendulum system using the known distance of

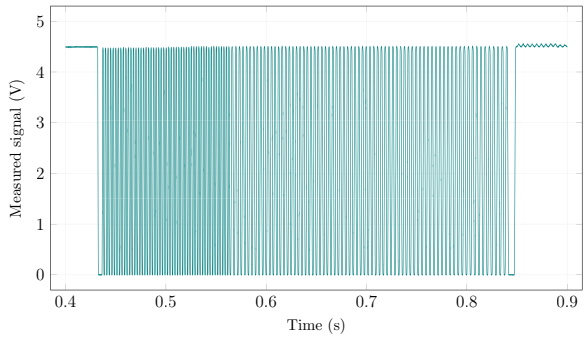

Fig. 6 An example of data acquired from one optical gate pair of the impactor's measuring device.

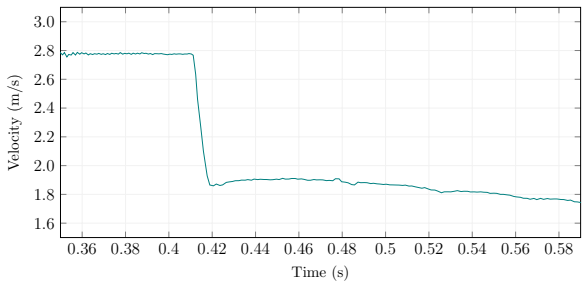

Fig. 7 The impactor's velocity calculated from acquired data.

the centre of rotation to the point where this velocity was measured. It was observed, that the differences between the resulting kinetic energies, calculated using these velocities, and the starting potential energies were negligible.

The after-impact velocity of the impactor is obtained similarly from the same data, but from averaging 10 to 20 partial velocities. This is necessary because after the impact, both the impactor and the specimen start oscillating, therefore, more averaging is needed to minimise the effect on the calculated velocity. However, it can be seen that the velocity starts noticeably decreasing approximately 0.05 s after the impact, so averaging must only be done on a reasonable number of partial velocities. Still, certain inaccuracy of the post-impact velocity would be present.

Using the optical gate approach, there is another way to determine the post-impact mechanical energy of the impactor. After the impact, the impactor is free to swing forward and back again through the optical gate. This means, that two sets of measurements will be acquired (one like in Fig. 6 and another one mirrored after it). If we pick one point on the comb-like attachment, for example, its back edge, then we can easily identify it in the measured signal. It will be the last point in the pass forward and the first point for backwards motion. The time interval between these two points can be easily identified. Again, this is done for all six of the photodiodes, so six of these time intervals are obtained.

The impactor must have reached the maximum of its trajectory in the middle of these time intervals. So this is considered time zero. Of course, certain mechanical energy is dissipated by the swing, but since we have measurements from six different points, we can compare them for both movements. It was observed that the velocities do not differ more than 0.5 %. So the assumption that the maximum point of the trajectory occurred in the middle of the intervals can be applied. In time zero, the angular displacement is unknown, but

the velocity is known because the impactor has stopped moving, also time is known. In the six points where measurement took place, the time and angular displacement are known, as that can be determined from the geometry of the relevant devices.

In the next step, we can use these known variables and fit onto them a theoretical curve of a pendulum motion. That is defined using the non-simplified equation

$$J\frac{d^2\theta}{dt^2} + MgC\sin\theta = 0, \tag{5}$$

where J is the moment of inertia of the whole pendulum system about the pivot point, θ is the angular displacement, M is the mass of the entire system and C is the distance between the centre of mass of the system and the pivot point. This equation is solved iteratively until it fits the measured data. The fit condition is chosen as lower than 0.1 % difference between the average angular displacement of the measured points and the corresponding points on the curve.

The fitted ideal curve (one half, for the backward motion) can be seen in Fig. 8. Even though all six measured points are shown there, only one is technically necessary for a successful calculation. It can be seen, that the fit is nearly perfect. This is because the physical pendulum equation was used and moment of inertia, mass and centre of mass position were determined. In a way, this is also a check that negligible mechanical energy is dissipated by the motion of the pendulum and that the pendulum's parameters were determined correctly, otherwise the fit could not be as good.

In the last step, the maximum angular displacement (at time zero) is easily identified from the theoretical curve and recalculated into the potential energy of the impactor. Based on experimental data, the mechanical energy obtained using this second approach is consistently slightly higher compared to the velocity measurement approach. This is correct, as the velocity approach truly must provide lower energies because of the inability to measure velocities immediately (in an infinitely small time interval) after the impact because of the oscillations. The second approach is, therefore, more precise, burdened only by the energy loses during the pendulum swings between the forward and backward measurements. But, as explained above, this effect is negligible. Similarly to the before-impact impactor energy, two approaches can be used simultaneously to prevent errors.

2.4 Measuring Technique—Specimen

The specimen is inside the two measuring frames during the whole experiment. The frames are designed to track its movement using a similar approach as outlined for the impactor. Pairs of optical gates made of laser modules (lower beams) and photodiodes (upper beams) are used. One frame has 50 gates. The first 20 are 3 cm apart, the rest are 5 cm apart. This is because it was assumed that for lower energy impacts, the specimen would not swing that far so more points would be beneficial towards the start. The electronics are set up so that all 50 photodiodes are part of a single measuring circuit using a summing amplifier. A voltage source is provided by a battery again. The output signal shows a sudden drop in voltage if one laser beam is interrupted and a sudden rise when it is illuminated again. An example of such a signal from one frame can be seen in Fig. 9.

This signal is first smoothed to remove any high-frequency noise as a result of the analogue to digital conversion. The sudden changes are then identified by applying a gradient function on the signal and identifying the gradient's peaks (for normal and inverted signals to identify both rises and drops). This yields the exact time points when the changes happened and they can be also seen in Fig. 9. The drops represent the front of the specimen, as that would be the part of the specimen that first interrupted a laser beam, and the back would then correspond to the rises. It is important to cut the raw signal when the specimen started moving backwards, as this imaginary order would be switched and the analysis would

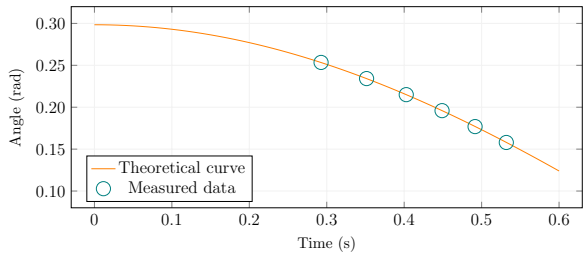

Fig. 8 The ideal curve fitted onto the measured data.

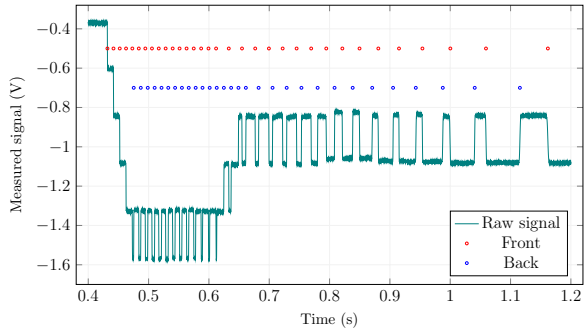

Fig. 9 The measured signal on one frame for tracking the specimen.

be unnecessarily complicated. In the raw signal, the approximate position of the specimen's peak trajectory is clearly visible, as that is an area with the largest distance between signal changes.

Before each experiment, the position of the specimen is measured relative to the frames. Since the geometry of the frames is known, then the position of the specimen relative to each optical gate can be calculated. These positions can then be used to obtain the corresponding angular displacement of the specimen's pendulum system. Next, this angular displacement can be paired with the previously analysed time points of the signal. The measuring frame tracks the front and the back of a cross-section of the specimen that is present in the plane defined by the frame. If we want to obtain tracking of this cross-section's centroid, then these two tracking sets need to be simply averaged. At this point, the peak of the trajectory is still unknown, as it occurred somewhere between two optical gates. Similarly to the calculations of the potential energy of the impactor, we can fit an ideal pendulum curve to this data and obtain that peak from it. The fitting process is similar to the impactor and an example of the result can be seen in Fig. 10. The difference is, that we only know the angular displacements and times of all the measured points (the first point is the initial point) but velocities are unknown.

This analysis yields two peaks of the angular displacement, one for each measuring frame. These two points can be averaged to obtain the peak for the specimen's centre of mass. When the specimen is still relatively undamaged and the main crack is small, then this simple calculation is accurate. However, when the crack is large and the specimen starts to significantly deform, the centre of mass would be identified incorrectly so a correction is applied based on the geometry of the specimen, its position in the frames and also the final angular displacement (because the specimen is also rotated together with the steel ropes, see Fig. 2).

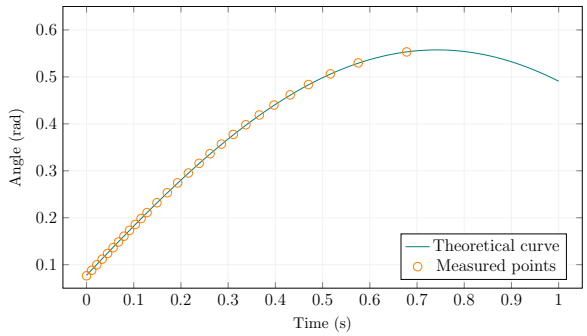

Fig. 10 The processed tracking of the specimen and fitted theoretical curve.

3 Experimental Programme

3.1 Materials

Using this new device, an experimental programme was carried out using 4 different concrete mixture designs, which are presented in Table 1. Intentionally, these designs are significantly different to obtain a general information regarding the mechanical performance of a broad range of materials. Material HSC is a high-strength concrete, which was used in study (Sovják et al. 2013). It is a relatively ordinary modern fibre-reinforced concrete. The second material DM (dry mixture) (Kolář et al. 2015; Kravanja et al. 2017) is a high-performance concrete, which is prepared in a commercial mixing plant and supplied to the laboratory as a dry mixture, which only requires the addition of water and fibres. The main aspects of this design are the use of fine aggregates only, good workability and the presence of silica fume which should offer a stronger matrix–fibre interface.

The last two materials were adapted to be used in the local conditions with the available constituents. The first one is material L (Luccioni et al. 2017), which is another high-performance concrete, but in this case, coarse aggregate is used. The last material R (Ranade et al. 2015) is an ultra-high performance concrete that uses fine aggregate only and very high amounts of cement and silica fume. Thanks to that, this material was able to accept the highest amount of reinforcing fibres while still retaining acceptable workability in the fresh state. Two types of fibres were used (Table 2) in various volumes and combinations.

Table 1 Mixtures summary. Adapted after Sovják et al. (2013); Kolář et al. (2015); Luccioni et al. (2017); Ranade et al. (2015), respectively.

Constituents	Mixtures			
	HSC	DM	L	R
Cement 42.5 R	1.00	1.00	1.00	1.00
Silica fume		0.10	0.10	0.39
Silica flour		0.25		0.28
Ground limestone			0.07	
Aggregate (mm)				
0.1/0.6				0.70
0.1/1.2		1.60		
0/4	3.05		0.67	
4/8	1.95		1.18	
HRWR[1]	0.01	0.01	0.013	0.02
Anti-foaming agent		0.001		
Water	0.46	0.1[2]	0.30	0.38

1 High-range water reducer

2 Relative to the dry mixture's weight

Table 2 Fibre volumetric contents. Fibres: S—straight 13 mm × 0.14 mm, H—hook-end 30 mm × 0.38 mm.

Mixture	Fibre type	
	S	H
HSC		0.50
		0.63
		1.00
L		0.50
		1.00
		1.50
R	2.00	
	3.00	
	4.00	
DM	1.00	
	1.50	
	2.00	
		1.50
	0.50	1.00
	1.00	0.50

3.2 Specimens

All the specimens manufactured for the experimental programme were beams 100 mm × 100 mm × 550 mm. The materials were mixed in a 70 l pan mixer. Water was added together with the high-range water-reducer. Fibres were slowly sprinkled into the mixture during mixing. Care was taken to place the fresh mixture only into the centre of the moulds. The material was free to flow to the rest of the volume either on its own or using vibration and manual compaction. It was important to use the same filling method for all specimens, as it limited the influence of the placement method on the orientation of fibres. Nevertheless, the varying orientation cannot be completely eliminated. The specimens were demoulded after 24 h and placed in a closed environment with high relative humidity for at least 27 days. For each mixture and fibre percentage and type, 9 specimens were made—135 in total.

A notch was cut into the centre of all specimens after the curing period ended. The notch was 30 mm deep, as recommended by the standard JCI-S-001-2003 (method of test for fracture energy of concrete by use of notched beam) (Japan Concrete Institute 2003). For the impact pendulum testing, the notched specimens were chosen based on previous experience. It was discovered, that under impact loading, specimens from the same sample developed significantly different damage patterns. Certain specimens, usually with higher percentages of fibres, cracked in various places around the centre span with the main crack propagating sometimes significantly far away from the centre. This was a variable, that made the comparison of the results problematic. A notch should unify the damage patterns. This is a compromise solution, as crack evolution is strain-rate sensitive and this approach partially removes its effect on the results.

Fig. 11 The three-point bending experiment for the quasi-static testing.

3.3 Quasi-Static Testing

The quasi-static testing was conducted using three-point bending experiments. Fig. 11 shows the setup. The span between supports was 500 mm and the load was applied in the centre of the beam, directly above the notch. Potentiometer displacement sensors were used to measure the displacement of the top surface. They were connected to a special fixture on both sides of the specimen. This fixture is attached to points in the centre of the specimen's height directly above the supports. On one side, it can slide on this attachment to accommodate the changing geometry of the specimen as the experiment progresses. The load is applied through an overlapping steel piece, which forms the reference surface for the potentiometers. The final displacement value was an average of the two measurements. The three-point configuration was chosen for better comparability with the impact experiments and because of using the notched specimens.

For later comparisons, the crack mouth opening displacement (CMOD, the width at the tip of the notch) values are needed. The CMOD values were not measured, as a specialised clip gauge was not available. The CMOD was calculated from the measured displacement instead. The experiment is carried out to a CMOD value of approximately 20 mm (limitation of the measuring apparatus). The force is recorded using a transducer in the loading piston. The total dissipated mechanical energy (for comparison with the impact experiments) was calculated as the area under the load–displacement curve.

3.4 Impact Testing Process and Analysis

At the start of the impact pendulum testing, the specimens are weighed and the CMOD is measured using

a digital calliper. The experiments are designed so that each specimen is loaded by approximately 10 consecutive impacts before it fails. This is done by changing the impactor's initial height based on the previous experience with the testing and the quasi-static performance. The heights are then fine-tuned during the experiment as well. After each impact, the CMOD is measured again.

A typical output of the experiment is then a cumulative sequence of dissipated energies paired with the corresponding CMOD, i.e. the dissipated energies are summed for each previous impact. The final dissipated energy values, which are presented in the following text, are then values for 20 mm CMOD. This is done so they can be compared to the quasi-static testing. The 20 mm energy value is obtained by fitting an ideal spline curve to the measured data and then reading the spline value for the needed CMOD. As mentioned above, the last impact, after which the specimen fails, cannot be measured as the specimen must remain in one piece for the tracking technique. However, highly damaged specimens have their energy absorbing capacity almost completely depleted, so not counting the last impact results in minimum inaccuracy. Besides, since the last impact occurs well above the chosen 20 mm CMOD mark, this is of no concern.

The initial impactor's height is modified during the experiment so that the largest CMOD values are reached before the specimen's complete failure and also to not have significant gaps in the CMOD values. It requires certain experience with the testing process, but it can also be estimated from the CMOD values. If a specimen experiences a much larger increase in CMOD compared to the previous impact, the initial height should be reduced, which also provides more experience for the next specimens.

The number of consecutive impacts was chosen arbitrarily to have sufficient data points, but also to limit the time consumption of the experiment. Choosing the right initial heights was done based on previous experience with the materials and the impact pendulum, but also based on the behaviour of the first specimen from one sample. Each specimen was tested using different initial heights based on its behaviour throughout the experiment to approximately maintain the total number of impacts. But it should be noted, that the changing impact velocity is still relatively similar and in the range of low-velocity impacts. This approach was chosen to fully deplete, in a controllable way, the energy dissipating (flexural) capacity.

4 Experimental Results and Discussion

4.1 Quasi-Static Experiments

The resulting dissipated energies from both the quasi-static and the impact experiments are summarised in Table 3 and shown in Fig. 12. Overall, the quasi-static testing revealed the basic behaviour of each material mixtures and fibre volumes. Starting from mixture HSC, it showed expected performance for the two lowest percentages, but the higher reinforcement of 1.0 % did not contribute to higher dissipated energy. Mixture L, on the other hand, showed a better ability to anchor and probably even disperse the same type of fibres, resulting in higher dissipated energy values. This is probably due to the higher cement content, the use of admixtures and

Table 3 Dissipated energies for both experiments. Numbers in brackets are the standard deviations.

Mixture	Fibres	Dissipated energy	
		Quasi-static test	Impact test
	(%)	(J)	
HSC	H 0.5	65.6 (9.1)	153.5 (19.0)
	H 0.63	74.9 (6.6)	191.0 (26.3)
	H 1.0	69.7 (9.7)	210.0 (40.7)
L	H 0.5	55.5 (8.9)	112.1 (17.1)
	H 1.0	82.7 (10.4)	189.1 (37.3)
	H 1.5	115.9 (12.2)	265.7 (59.3)
DM	S 1.0	47.3 (4.3)	136.6 (13.8)
	S 1.5	60.5 (4.1)	176.7 (14.9)
	H 1.5	137.1 (10.9)	378.0 (40.4)
	H 1.0 + S 0.5	125.3 (15.5)	342.7 (54.3)
	H 0.5 + S 1.0	108.9 (7.6)	285.1 (56.6)
	S 2.0	105.1 (8.4)	257.6 (6.6)
R	S 2.0	103.7 (9.8)	305.3 (60.7)
	S 3.0	154.5 (4.6)	426.1 (46.4)
	S 4.0	123.1 (20.7)	458.6 (28.1)

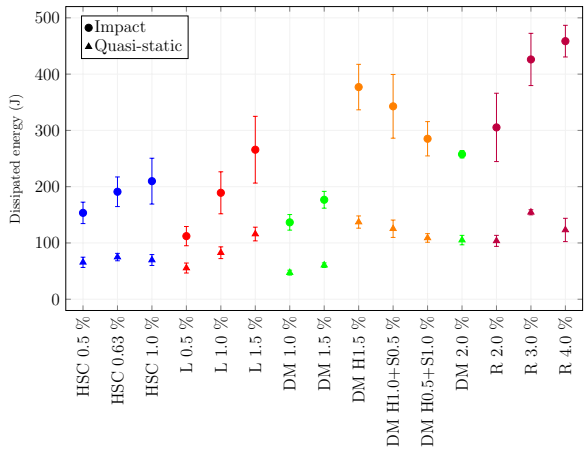

Fig. 12 Dissipated energies for the quasi-static and impact experiments.

lower amount of coarse aggregate. Also, mixture L had better workability with 1.5 % than mixture HSC with only 1.0 % indicating overall better optimisation of the mixture to accept fibre reinforcement.

Mixture DM continued this trend of better performance with the same hook-ended fibres. This is logical as this mixture contained even more cement, admixtures and lower aggregate size. However, the performance with the short straight fibres was worse. The combined fibre specimens then showed expected performance proportional to the fibre mix. The straight fibres were used for the mixture R as well. For the 2 % fibre volume, the results were comparable between the mixtures R and DM. The highest values were observed for the 3 % specimens. Similarly to the mixture HSC, the mixture R probably had a fibre-saturation point between the two highest percentages of fibres tested, as the 4 % specimens showed worse performance compared to the 3 %.

From the bending experiments' point of view, mixture L performed the best taking into consideration the composition of the material (its cost). As expected, the mixture DM showed the best spread of the results for the straight fibres, as there could have been more of them for a given volume due to their smaller size, so achieving better homogeneity was easier. Especially the energy dissipation for the hook-ended fibres showed a worse spread of the results, partially due to the lower fibre count, but probably also due to the damage to the matrix. During the pullout of a hook-end fibre, there was an increased risk of premature matrix failure. If that happened, the fibre lost bond to the matrix which led to a faster decay of force during the experiment.

4.2 Impact Experiments

It can be immediately seen in Fig. 12, that the results for the impact experiments have similar trends, although certain key differences are present. On one hand, this is a clear indication of the suitability of the impact measuring principle, since the trends are not vastly different. On the other hand, the differences in trends should indicate the strain-rate related effects. Right at the start, it is important to understand and take into consideration the different loading methods between the experiments. Certain reference results would be needed to know the exact difference between the impact pendulum and bending experiments without the influence of strain rate. That is of course not possible, as we cannot load a specimen in the impact pendulum using a quasi-static loading rate nor can we load the beam in the exact same bending setup using an impact rate. That is the reason authors do not want to present these values as relative ratios using, for example, the dynamic increase factor (DIF).

It should then be stressed that the impact experiments serve a comparative purpose. The main focus is on identifying trends regarding different fibre reinforcement and mixture designs and analysing the differences in these trends between the quasi-static and impact experiments. The only difference between the individual impact pendulum tests was the changing initial height of the impactor. But based on the literature overview (Pajak 2011), the strain-rate effects in the region of low-velocity impact loading significantly change only between orders of magnitude of the applied strain rate. The initial heights of the impactor ranged from 0.15 m to 0.60 m depending on the specimen. This translates to approximately 2.0 m/s and 8.3 m/s impact velocity. For highly damaged specimens in later stages of the experiment, initial heights towards the lower range were used as needed.

The comparison between the mixtures HSC and L is especially interesting, as both of these mixtures contained the same fibre types and aggregate size, but mixture L contained more cement and admixtures. This made the mixture L perform better than mixture HSC under quasi-static conditions, at least for the 1 % fibre content and up. But the impact loading results between mixtures HSC and L were comparable. A possible theory behind this behaviour could be, that the fibres were anchored better in the matrix L thanks to its composition, but overall, the tensile strength of matrix L was not much higher compared to matrix HSC, so premature fibre-matrix failure occurred in matrix L more often than in matrix HSC. This effect could have been amplified by the higher strain rate. Strong evidence for this are the final shapes of the fibres. Mixture HSC showed almost all fibres straightened, which indicates a complete pullout, while some fibres on the failure surfaces of specimens L still showed the hook-ends, especially the 1.5 % L specimens.

The mixture DM exhibited relatively high increase of dissipated energy for the two lowest percentages of straight fibres while achieving the lowest increase for the highest percentage. Adding hook-ended fibres resulted in apparently lower strain-rate sensitivity in this mixture, although still higher compared to mixture L. This could also be explained by the aforementioned theory because the hook-ended fibres at the failure surfaces of specimens DM showed a higher number of fibres straightened, so complete pullout was achieved together with high energy dissipation.

Comparing the mixtures DM and R, we can observe higher performance of R with the same 2.0 % fibre volume. This might also indicate higher strain-rate sensitivity of this particular combination of matrix and fibre. It could also mean, that since matrix R should be stronger and able to anchor the fibres better, it will achieve better single fibre performance. However, this effect seems to

prevail only during higher strain-rate loading. In the case of 4.0 % reinforcement, there is a significant difference between the experiments. This trend is similar to mixture HSC, where the highest percentage also achieved higher dissipated energy. This observation could be linked to the nature of strain-rate related damage patterns. If a crack is initiated in a low fibre volume specimen, then the crack is already the weakest link of the composite so it keeps growing until failure. In a high fibre volume composite, the formation of a crack does not necessarily create the weakest point, as the fibres are able to transfer the tensile stresses through the crack. This means that another crack can easily be initiated elsewhere, or the main crack could start branching, which all leads to higher energy dissipation. This effect is clearly strain-rate sensitive. Additionally, all of the specimens tested on the impact pendulum were subjected to the effects of strain-rate sensitive matrix damage, mostly in the direct proximity of the reinforcing fibres.

4.3 Impact Pendulum Evaluation

During the design, assembling and testing of the impact pendulum apparatus, together will all the measuring devices, several key technical aspects were identified. These aspects should be considered for possible replication of this experimental setup. First, the rigidity of the entire structure plays an important role. Ideally, the impactor should be connected to a separate structure. When the impactor is released from its initial height, the reaction forces from the cable attachments cause a slight deflection and vibration of the structure, which can be picked up by the measuring instruments and negatively affect results.

The length of the cable suspensions should be as long as possible. In this case, the lengths were approximately 2.5 m, which proved to be sufficient. This length limits the maximum lifting height of the impactor, depending on the attachment and lifting mechanism. In our case, using the horizontal electromagnetic lock, exceeding 1.5 m lifting height was unreliable and introduced high mechanical shock to the cables upon release. But since in these experiments the initial height did not exceed 0.6 m, this issue was eliminated. Another consideration regarding the lengths relates to the velocities measurements. The impactor, right before the impact, is considered to be moving horizontally for the velocity calculation based on its passage through the optical gates. This simplification is only possible because of the relatively long cables.

The hardness of the impactor's front is important. During the previous testing on the impact pendulum it was discovered, that after numerous impacts the front can exhibit plastic deformation. Even though it was most probably small during individual impacts, it was difficult to estimate the related energy losses. Using the new hardened steel nose (which is also replaceable) is beneficial in this regard. No damage was observed on the impactor after the entire experimental campaign (roughly 750 impacts).

Tracking of the specimen was done using the laser modules and photodiodes. It was thought that a higher density is needed towards the start of the motion, so 3 cm spacing was used. However, when the specimen started rotating after the impact, its horizontal projection reached close to 12 cm, which is a multiple of the spacing. This means, that immediately when a laser beam is interrupted, another one is illuminated again. The measured signal then either shows just a small spike or no change at all. However, if the tracking apparatus is to be universal for different specimen sizes, this is inevitable. Nevertheless, it did not prevent a successful analysis of the signal.

The laser beam modules on the lower beams were firmly glued into their positions. The manufacturer of the modules states a certain allowed tolerance for the deflection of the beam from the axis of the module housing. It was discovered, that this tolerance is rather high, and each module needed to be carefully oriented before glueing to achieve proper aim towards the photodiodes on the upper beams. Ideally, each of the laser modules should have been placed in a mechanism that would allow further alignment and subsequent firm locking. Disassembling of the measuring frames (to make way for a different experiment on the impact pendulum) and repeated assembling now requires careful and time-consuming alignment of the whole structure, including precise tightening of the bolted connections, adding washers and shims. All of this while monitoring the photodiodes' circuit signal level, to achieve the lowest possible base voltage on both frames at the same time. An alternative to this would be a measuring frame welded into one piece. Although this would require more space for storage and more accurate manufacturing tolerances.

Regarding the ease of conducting the experiments and data analysis, the impact pendulum and the measuring frames performed adequately. Through many improvements of the measuring frames' structure, optical elements positioning and electronics, the data acquisition process became reasonably reliable and resulted in easy-to-analyse data sets.

The data analysis was conducted by a computer script in a MATLAB environment, which was technically not part of the impact pendulum. Overall, the analysis was possible thanks to the quality of the acquired data, i.e. the clear presence of the voltage peaks, drops and rises, good signal-to-noise ratios and sufficient speed of data acquisition. However, the analysis was still performed without complete automation, as the script required manual

inputs and checks. Ideally, custom software would need to be created (and perhaps even processing hardware as part of the impact pendulum) that would show the resulting dissipated energies right after the impact. This was beyond the scope of this work and the author's specialisation. Such automation would also require more sophisticated ways to automatically deal with potential inconsistencies in the obtained data, such as missing peaks or other errors.

The main principle behind the energy approach required the assumption that no other energy losses occur during the impact. The acoustic energy loss is immediately apparent. It is unclear how much energy is consumed for the acoustic effect, which is simply a transfer of a certain part of mechanical energy into the surrounding medium. Inside the specimen, a portion of the mechanical energy is dissipated as heat, as the main energy dissipating mechanism is the fibre-matrix friction. Another loss can be attributed to the inevitable compressive deformation and damage of the specimen in the contact region with the impactor. However, all of these energy losses related to the specimen can be interpreted as inseparable parts of the material performance, as they would be present even in a real high strain-rate loading situation. The rest of the losses regarding the impactor or the apparatus' structure are considered negligible.

4.4 Conclusions

Overall, the impact pendulum testing provides a reliable and relatively quick way of testing fibre-reinforced concretes for their ability to dissipate mechanical energy when subjected to an elevated strain-rate load. The energy approach seems more suited as an evaluating quantity, compared to the standard load/strength approach of the quasi-static testing. The detailed technical aspects of the impact pendulum were described throughout the paper for possible replication. However, to summarise and highlight the advantages, the most important are the absence of fixed supports, elimination of variables related to fixed supports, introduction of contactless measuring methods, speed and accuracy of data acquisition and subsequent analysis and relative simplicity of the whole system. The last point is also related to the cost, as the measuring devices use affordable electronic elements and the whole impact pendulum is a simple steel structure, which could be simplified further.

Laboratory testing such as this is intended for preliminary comparative testing when conducting basic material research. But for specific applications, other testing methods, or preferably the full-scale real loading scenarios, should be employed. An example of this would be ballistic or blast testing. The whole process of creating a better material is then an iteration using the obtained experience.

In terms of the experimental campaign of this work, the focus was on a broader range of materials with various fibre volumes. This allowed us to obtain more general results which gave us the material performance information when compared to the quasi-static behaviour. It was discovered that higher volumes of fibres showed the highest increases in the absorbed mechanical energies, i.e. higher strain-rate sensitivity. The damage of the matrix also played a major role, as stronger matrices anchored the fibres better. This behaviour was also strain-rate sensitive. Last but not least, the experimental campaign also served as a final test of the experimental approach.

Acknowledgements
Not applicable.

Authors' contributions
PK contributed to this study by assembling and testing of the impact pendulum device, conducted and analysed the experiments and prepared the manuscript; RS contributed to the conception of the project, secured funding, administrated the project and helped with writing the manuscript. All authors read and approved the final manuscript.

Authors' information
Petr Konrád researcher at the Experimental centre, Czech Technical University in Prague, Faculty of Civil Engineering, Thákurova 7, Prague 6 16629, Czech Republic, petr.konrad@fsv.cvut.cz. Radoslav Sovják associate professor at the Experimental centre, Czech Technical University in Prague, Faculty of Civil Engineering, Thákurova 7, Prague 6 16629, Czech Republic, sovjak@fsv.cvut.cz.

Funding
This study was supported by the Technology Agency of the Czech Republic (Grant number FW03010141).

Availability of data and materials
All data generated or analysed during this study are included in this published article.

Declarations

Competing interests
The authors declare that they have no competing interests.

Received: 16 December 2021 Accepted: 23 February 2022
Published online: 24 May 2022

References

Bede, N., Ožbolt, J., Sharma, A., & İrhan, B. (2015). Dynamic fracture of notched plain concrete beams: 3D finite element study. *International Journal of Impact Engineering, 77*, 176–188. https://doi.org/10.1016/j.ijimpeng.2014.11.022https://linkinghub.elsevier.com/retrieve/pii/S0734743X14002905.

Cao, Y., Yu, Q., Brouwers, H., & Chen, W. (2019). Predicting the rate effects on hooked-end fiber pullout performance from Ultra-High Performance Concrete (UHPC). *Cement and Concrete Research, 120*, 164–175. https://doi.org/10.1016/j.cemconres.2019.03.022https://linkinghub.elsevier.com/retrieve/pii/S0008884618309608.

Heravi, A. A., Curosu, I., & Mechtcherine, V. (2020). A gravity-driven split Hopkinson tension bar for investigating quasi-ductile and strain-hardening cement-based composites under tensile impact loading. *Cement and Concrete Composites*. https://doi.org/10.1016/j.cemconcomp.2019.103430. https://linkinghub.elsevier.com/retrieve/pii/S0958946519312739.

Janda, T., Zemanová, A., Hála, P., Konrád, P., & Schmidt, J. (2020). Reduced order model of glass plate loaded by low-velocity impact. *International Journal of Computational Methods and Experimental Measurements, 8*(1), 36–46. https://doi.org/10.2495/CMEM-V8-N1-36-46http://www.witpress.com/doi/journals/CMEM-V8-N1-36-46.

Japan Concrete Institute JCI-S-001-2003 (2003). Method of test for fracture energy of concrete by use of notched beam

Khosravani, M. R., & Weinberg, K. (2018). A review on split Hopkinson bar experiments on the dynamic characterisation of concrete. *Construction and Building Materials, 190*, 1264–1283. https://doi.org/10.1016/j.conbuildmat.2018.09.187https://linkinghub.elsevier.com/retrieve/pii/S095006181832378X.

Kolář, K., Bažantová, Z. & Konvalinka, P. (2015). Czech Patent 306 663: Suchá prefabrikovaná směs multifunkčního silikátového kompozitu.

Kravanja, S., Sovják, R., Konrád, P., & Zatloukal, J. (2017). Penetration Resistance of Semi-infinite UHPFRC Targets with various Fiber Volume Fractions against Projectile Impact. *Procedia Engineering, 193*, 112–119. https://doi.org/10.1016/j.proeng.2017.06.193https://linkinghub.elsevier.com/retrieve/pii/S1877705817327418.

Luccioni, B., Isla, F., Codina, R., Ambrosini, D., Zerbino, R., Giaccio, G., & Torrijos, M. (2017). Effect of steel fibers on static and blast response of high strength concrete. *International Journal of Impact Engineering, 107*, 23–37. https://doi.org/10.1016/j.ijimpeng.2017.04.027https://linkinghub.elsevier.com/retrieve/pii/S0734743X16300562.

Min, F., Yao, Z., & Jiang, T. (2014). Experimental and Numerical Study on Tensile Strength of Concrete under Different Strain Rates. *The Scientific World Journal, 2014*, 1–11. https://doi.org/10.1155/2014/173531http://www.hindawi.com/journals/tswj/2014/173531/.

Othman, H. & Marzouk, H. (2016). Strain Rate Sensitivity of Fiber-Reinforced Cementitious Composites. ACI Materials Journal. https://doi.org/10.14359/51688461.http://www.concrete.org/Publications/InternationalConcreteAbstractsPortal.aspx?m=details&i=51688461

Ožbolt, J., Sharma, A., İrhan, B., & Sola, E. (2014). Tensile behavior of concrete under high loading rates. *International Journal of Impact Engineering, 69*, 55–68. https://doi.org/10.1016/j.ijimpeng.2014.02.005https://linkinghub.elsevier.com/retrieve/pii/S0734743X14000360.

Pajak, M. (2011). The influence of the strain rate on the strength of concrete taking into account the experimental techniques. *Architecture Civil Engineering Environment, 4*(3), 77–86.

Ranade, R., Li, V. C., & Heard, W. F. (2015). Tensile Rate Effects in High Strength-High Ductility Concrete. *Cement and Concrete Research, 68*, 94–104. https://doi.org/10.1016/j.cemconres.2014.11.005https://linkinghub.elsevier.com/retrieve/pii/S0008884614002324.

Sadraie, H., Khaloo, A., & Soltani, H. (2019). Dynamic performance of concrete slabs reinforced with steel and GFRP bars under impact loading. *Engineering Structures, 191*, 62–81. https://doi.org/10.1016/j.engstruct.2019.04.038https://linkinghub.elsevier.com/retrieve/pii/S0141029618340513.

Sovják, R., Vavřiník, T., Máca, P., Zatloukal, J., Konvalinka, P., & Song, Y. (2013). Experimental Investigation of Ultra-high Performance Fiber Reinforced Concrete Slabs Subjected to Deformable Projectile Impact. *Procedia Engineering, 65*, 120–125. https://doi.org/10.1016/j.proeng.2013.09.021https://linkinghub.elsevier.com/retrieve/pii/S1877705813015282.

Tran, T. K., & Kim, D. J. (2012). Strain Energy Frame Impact Machine (SEFIM). *Journal of Advanced Concrete Technology, 10*(3), 126–136. https://doi.org/10.3151/jact.10.126http://joi.jlc.jst.go.jp/JSTJSTAGE/jact/10.126?from=CrossRef.

Vegt, I. & Weerheijm, J. (2016). Influence of moisture on the fracture behaviour of concrete loaded in dynamic tension. In: Proceedings of the 9th international conference on fracture mechanics of concrete and concrete structures. IA-FraMCoS. https://doi.org/10.21012/FC9.167. http://framcos.org/FraMCoS-9/Full-Papers/167.pdf.

Vivas, J., Zerbino, R., Torrijos, M., & Giaccio, G. (2020). Effect of the fibre type on concrete impact resistance. *Construction and Building Materials, 264*, 120200. https://doi.org/10.1016/j.conbuildmat.2020.120200https://linkinghub.elsevier.com/retrieve/pii/S0950061820322054.

Wu, M., Chen, Z., & Zhang, C. (2015). Determining the impact behavior of concrete beams through experimental testing and meso-scale simulation: I. *Drop-weight tests. Engineering Fracture Mechanics, 135*, 94–112. https://doi.org/10.1016/j.engfracmech.2014.12.019https://linkinghub.elsevier.com/retrieve/pii/S0013794414004159.

Xu, M., Hallinan, B., & Wille, K. (2016). Effect of loading rates on pullout behavior of high strength steel fibers embedded in ultra-high performance concrete. *Cement and Concrete Composites, 70*, 98–109. https://doi.org/10.1016/j.cemconcomp.2016.03.014https://linkinghub.elsevier.com/retrieve/pii/S0958946516300518.

Yoo, D. Y., Chun, B., & Kim, J. J. (2019). Effect of calcium sulfoaluminate-based expansive agent on rate dependent pullout behavior of straight steel fiber embedded in UHPC. *Cement and Concrete Research, 122*, 196–211. https://doi.org/10.1016/j.cemconres.2019.04.021https://linkinghub.elsevier.com/retrieve/pii/S0008884618314030.

Yu, R., van Beers, L., Spiesz, P., & Brouwers, H. (2016). Impact resistance of a sustainable Ultra-High Performance Fibre Reinforced Concrete (UHPFRC) under pendulum impact loadings. *Construction and Building Materials, 107*, 203–215. https://doi.org/10.1016/j.conbuildmat.2015.12.157https://linkinghub.elsevier.com/retrieve/pii/S095006181530828X.

Publisher's Note